Nanoscale Research Letters
a SpringerOpen Journal

NANO EXPRESS   **Open Access**

Improvement of optical transmittance and electrical properties for the Si quantum dot-embedded ZnO thin film

Kuang-Yang Kuo, Chuan-Cheng Liu, Pin-Ruei Huang, Shu-Wei Hsu, Wen-Ling Chuang, You-Jheng Chen and Po-Tsung Lee[*]

Abstract

A Si quantum dot (QD)-embedded ZnO thin film is successfully fabricated on a p-type Si substrate using a ZnO/Si multilayer structure. Its optical transmittance is largely improved when increasing the annealing temperature, owing to the phase transformation from amorphous to nanocrystalline Si QDs embedded in the ZnO matrix. The sample annealed at 700°C exhibits not only high optical transmittance in the long-wavelength range but also better electrical properties including low resistivity, small turn-on voltage, and high rectification ratio. By using ZnO as the QDs' matrix, the carrier transport is dominated by the multistep tunneling mechanism, the same as in a n-ZnO/p-Si heterojunction diode, which clearly differs from that using the traditional matrix materials. Hence, the carriers transport mainly in the ZnO matrix, not through the Si QDs. The unusual transport mechanism using ZnO as matrix promises the great potential for optoelectronic devices integrating Si QDs.

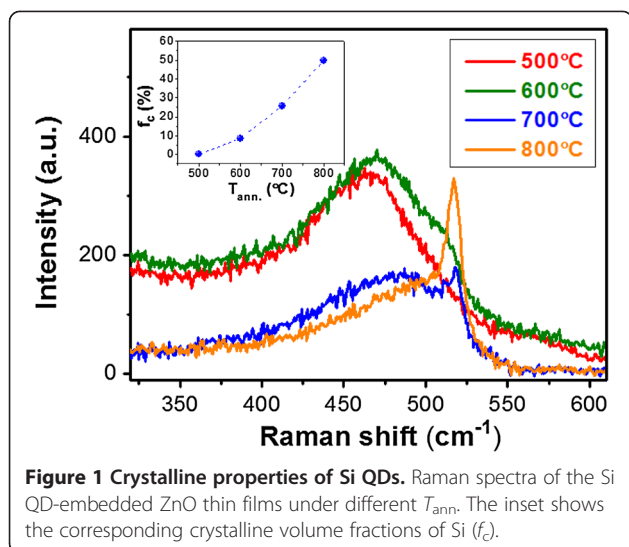**Keywords:** Si quantum dot; ZnO thin film; Transport mechanism

Background

Recently, Si quantum dots (QDs) embedded in traditional Si-based dielectric matrix materials like SiO_2 and Si_3N_4 have been extensively studied and successfully applied to various optoelectronic devices [1-3], owing to their many unique characteristics such as highly tunable bandgap and better optical properties [4-6]. In particular, Si QD is persistently considered as a candidate for next-generation light emitters in Si photonics because of its greatly improved internal and external quantum efficiencies [7,8]. To further improve the device performance, utilization of Si-rich Si-based dielectric materials as Si QDs' matrices has also been developed [9,10]. A suitable matrix material for Si QDs is very important for better device performance. We propose to embed Si QDs into a ZnO thin film because ZnO has many desirable features to function as Si QDs' matrix material, e.g., wide and direct bandgap, high transparency, and highly tunable electrical properties [11]. Hence, ZnO can serve as the Si QDs' matrix to achieve bandgap engineering,

reduce the optical loss from the matrix's absorption, and efficiently enhance the carrier transport efficiency for optoelectronic device application. The fabrication and fundamental optical properties of the Si QD-embedded ZnO thin films have been reported in our previous works [12,13]. In this study, improvement of optical transmittance and electrical properties of the Si QD-embedded ZnO thin films is investigated and discussed.

Methods

The ZnO/Si multilayer (ML) thin films with 20 bilayers are deposited on p-type Si (100) substrates or fused quartzes at room temperature using the radio-frequency (RF) magnetron sputtering method. The sputtering powers of ZnO and Si are fixed at 75 and 110 W, and the effective thicknesses of each ZnO and Si layer are fixed at 5 and 3 nm, respectively. After deposition, the ZnO/Si ML thin films are annealed at 500°C, 600°C, 700°C, or 800°C for 30 min in N_2 environment. For electrical measurements, 100-nm-thick Al and Ni metal layers are deposited on the top and bottom surfaces of devices as electrodes using a thermal coater. The Raman spectra are measured using a 488-nm diode-pumped solid-state laser (HORIBA LabRam HR,

* Correspondence: potsung@mail.NCTU.edu.tw
Department of Photonics and Institute of Electro-Optical Engineering, National Chiao Tung University, 1001 Ta-Hsueh Road, Hsinchu 30010, Taiwan

Springer

Figure 1 Crystalline properties of Si QDs. Raman spectra of the Si QD-embedded ZnO thin films under different T_{ann}. The inset shows the corresponding crystalline volume fractions of Si (f_c).

HORIBA, Kyoto, Japan). The X-ray diffraction (XRD) patterns are examined by a Bede-D1 X-ray diffractometer with Cu Kα radiation (Bede Scientific, Engelwood, CO, USA). The transmittance spectra are obtained using a UV–vis-NIR spectrophotometer (Hitachi U-4100, Hitachi Ltd., Chiyoda, Tokyo, Japan). The cross-sectional morphologies are observed by a JSM-6500 F field-emission scanning electron microscope (SEM; JEOL Ltd., Akishima, Tokyo, Japan). The current–voltage (*I-V*) curves are measured using an Agilent E5270B precision measurement mainframe (Agilent Technologies Inc., Santa Clara, CA, USA).

Results and discussion

In our previous works, we demonstrated that a high Si sputtering power can assist the formation of the self-aggregated amorphous Si QDs embedded in the ZnO matrix during deposition by utilizing a ZnO/Si ML structure [12]. In order to investigate the crystalline properties of the Si QDs embedded in ZnO thin films under different annealing temperatures (T_{ann}) for a longer annealing duration, Raman spectra are measured and shown in Figure 1.

Generally, the signal of Si materials can be decomposed into three components including the peaks located at approximately 480, 500 ~ 510, and 510 ~ 520 cm^{-1}, which originated from the transverse optical (TO) modes of Si-Si vibrations in the amorphous (a-Si), intermediate (i-Si), and nanocrystalline Si (nc-Si) phases [14]. The corresponding crystalline volume fractions of Si (f_c) obtained from fitting the curves are shown in the inset of Figure 1 [14]. The nc-Si phase is formed in the ZnO matrix and significantly increased by increasing T_{ann} when T_{ann} is higher than 600°C. This indicates that a higher T_{ann} can largely enhance the crystalline quality of Si QDs embedded in the ZnO matrix.

Since the crystalline properties of the ZnO matrix can influence its optical and electrical properties [15], the XRD patterns of the Si QD-embedded ZnO thin films annealed at different temperatures are examined and shown in Figure 2a, fine-scanned from 30° to 40°. A main diffraction signal is observed at approximately 34.5° for all the samples. As shown in Figure 2b and its inset, this signal can be decomposed into two components in Gaussian form with peaks located at about 34.3° and about 36.3°, which are contributed from (002) and (101) orientations of ZnO [16]. In Figure 2a, the crystallization intensity of the ZnO matrix is slightly reduced when increasing T_{ann}. This may be due to the increased interior film stress resulting from the phase transformation of a- to nc-Si QDs. From the results of Raman and XRD measurements, we show that the nc-Si QDs embedded in the crystalline ZnO matrix can be achieved by a T_{ann} higher than 600°C.

The optical transmittance spectra of the Si QD-embedded ZnO thin films under different T_{ann} are shown in Figure 3. The transmittance in the long-wavelength (long-λ) range (>600 nm) clearly increases when increasing T_{ann}. Since higher T_{ann} can obviously enhance the crystallization of Si QDs, the improved optical transmittance in the long-λ range can be attributed to the decreased absorbance from a-Si QDs due to the increased f_c of Si QDs [5]. It is worthy to note that high transmittance of approximately 90% in the long-λ range under a T_{ann}
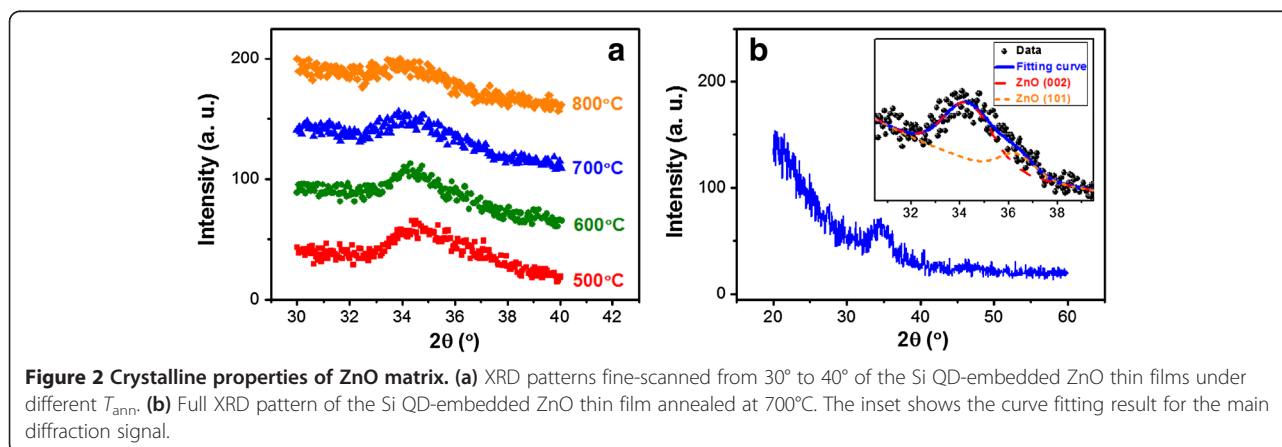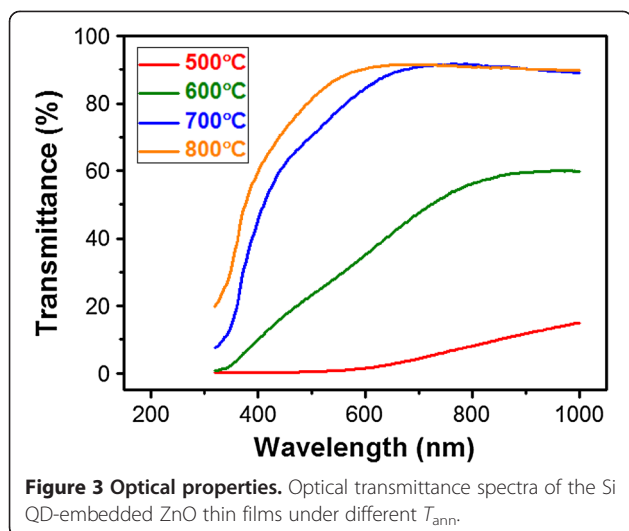

Figure 2 Crystalline properties of ZnO matrix. (a) XRD patterns fine-scanned from 30° to 40° of the Si QD-embedded ZnO thin films under different T_{ann}. **(b)** Full XRD pattern of the Si QD-embedded ZnO thin film annealed at 700°C. The inset shows the curve fitting result for the main diffraction signal.

Figure 3 Optical properties. Optical transmittance spectra of the Si QD-embedded ZnO thin films under different T_{ann}.
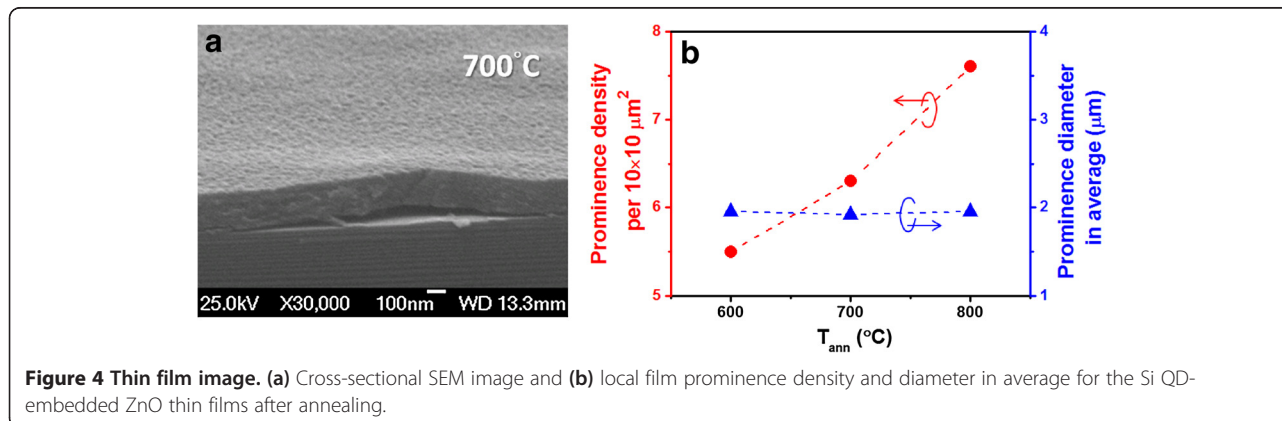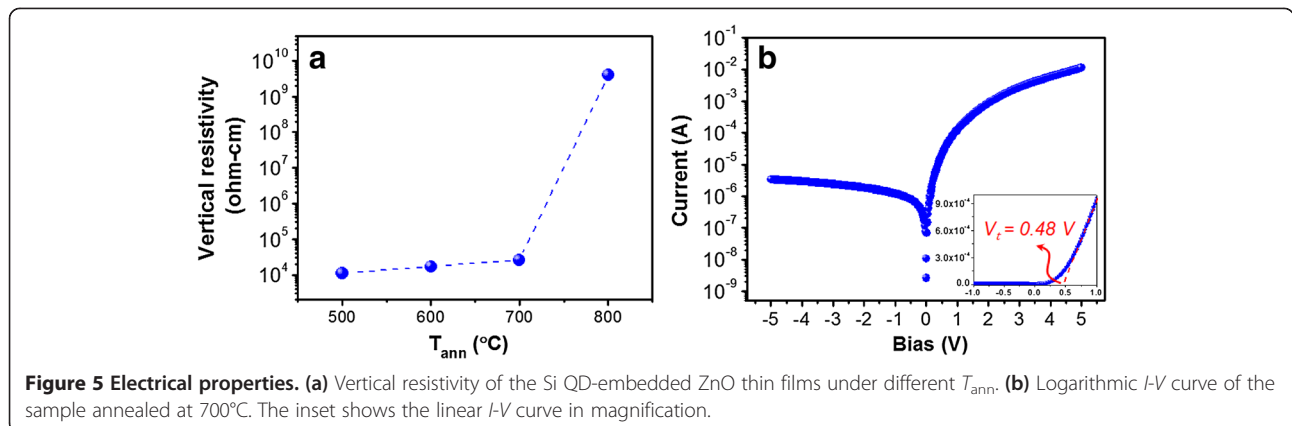
higher than 700°C can be achieved and is close to those using the traditional matrix materials [5]. From the above results, it is clear that better crystallization of Si QDs in the ZnO matrix is required to decrease the absorption from a-Si QDs and thus efficiently reduce the optical loss in the long-λ range for better optoelectronic device performance. We find that a high-enough T_{ann} for the Si QD-embedded ZnO thin film is critical to significantly improve the optical properties.

The images of the Si QD-embedded ZnO thin films after annealing are examined by SEM. The local film prominences are observed when T_{ann} is higher than 600°C. Figure 4a shows the cross-sectional SEM image of a sample annealed at 700°C. The local film prominence density and diameter in average are estimated and shown in Figure 4b. The prominence density increases almost linearly from 5.5 to 7.6 ones per 10×10 μm^2 when increasing T_{ann} from 600°C to 800°C with a close average diameter of about 2 μm. According to Raman spectra, the phase transformation of a- to nc-Si QDs happens when T_{ann} is larger than 600°C, and f_c also increases with

increasing T_{ann} from 600°C to 800°C. This strong correlation between f_c and prominence density means that the volume variation from the phase transformation of a- to nc-Si QDs embedded in the ZnO matrix during annealing can produce an interior film stress and lead to the occurrence of local film prominences.

To understand the electrical properties of the Si QD-embedded ZnO thin films, the vertical resistivity (ρ) is calculated from the slope of the I-V curve under a high forward bias region of $4 \sim 5$ V. When increasing T_{ann}, the ρ can be reduced by the improved crystalline quality of Si QDs but also raised by the increased film prominence density and degraded crystalline quality of the ZnO matrix. Figure 5a shows the obtained ρ under different T_{ann}, which slightly increases when increasing T_{ann} from 500°C to 700°C but still keeps a low resistivity of approximately 10^4 Ω cm, significantly lower than that (approximately 10^8 Ω cm) of the intrinsic Si QDs embedded in a SiO$_2$ matrix [17,18]. It is evident that using ZnO as matrix can overcome the issue of highly resistive nature of the traditional Si-based dielectric matrix materials, and 10^4 times improvement of ρ is obtained. The ρ largely increases for the sample annealed at 800°C, which may have resulted from the excess film prominences produced during annealing since the film prominences will lead to local broken circuit regions at the interface of film/substrate and significantly increase the resistivity. Hence, we can conclude that annealing at 700°C is a more suitable annealing condition to have better crystallization of Si QDs in the crystalline ZnO matrix, low ρ, and high transmittance in the long-λ range. The logarithmic I-V curve of the sample annealed at 700°C is shown in Figure 5b, and its inset shows the corresponding linear I-V curve in magnification. It clearly exhibits not only a good rectification ratio of 3.4×10^3 at ±5 V but also a low turn-on voltage (V_t) of 0.48 V, which agrees with the reported results of the n-ZnO/p-Si heterojunction (HJ) diode [19,20]. Even though the Si QDs are embedded in the ZnO matrix, we show that the fabricated ZnO thin film on p-Si can still
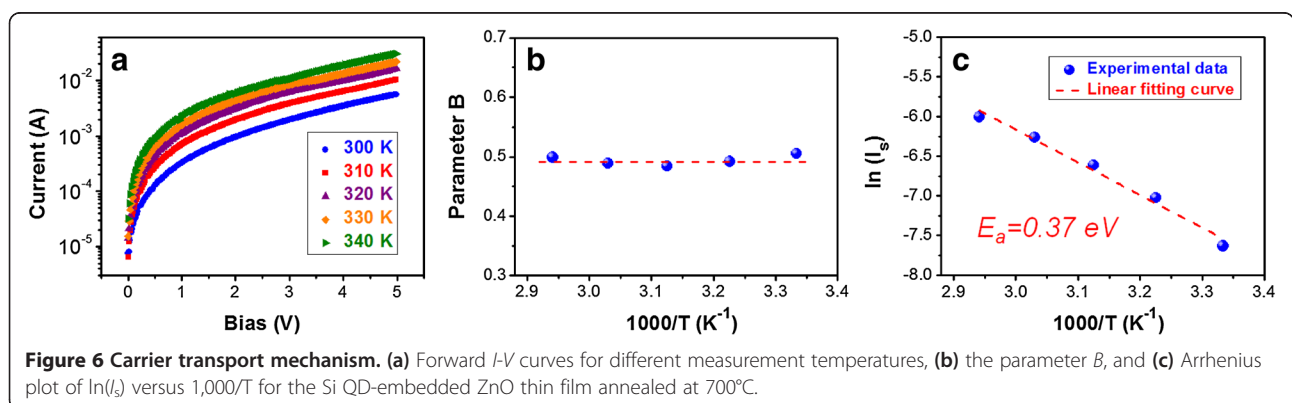

Figure 4 Thin film image. (a) Cross-sectional SEM image and **(b)** local film prominence density and diameter in average for the Si QD-embedded ZnO thin films after annealing.

Figure 5 Electrical properties. (a) Vertical resistivity of the Si QD-embedded ZnO thin films under different T_{ann}. **(b)** Logarithmic *I-V* curve of the sample annealed at 700°C. The inset shows the linear *I-V* curve in magnification.

possess good p-n HJ diode behavior with large rectification ratio and low V_t.

To investigate the carrier transport mechanism, the temperature-dependent forward *I-V* curves of the sample annealed at 700°C are examined and shown in Figure 6a. The *I-V* curves exhibit the typical temperature dependence of a p-n junction diode. The current clearly increases as we raise the measurement temperature (T_{meas}). In the low bias region (smaller than approximately 0.5 V), the currents can be well fitted to be proportional to about $V^{1.2}$ for different T_{meas}, which slightly deviates from the ohmic behavior. This means that the surface states and/or an inherent insulating SiO_2 thin layer at the interface of the n-ZnO matrix/p-Si substrate has influence on the transport of carriers [21]. In the high bias region (larger than approximately 0.5 V), the forward currents can be well expressed by $I = I_s[\exp(BV) - 1]$ for different T_{meas}, where I_s is the reverse saturation current and parameter B is a coefficient dependent or independent on temperature decided by the dominant carrier transport mechanism [21,22]. The fitted results for parameter B are shown in Figure 6b, which reveal that the parameter B is almost invariant for different T_{meas}. This independence of T_{meas} indicates that the carrier transport is dominated by the multistep tunneling mechanism,

which had been reported by Zebbar et al. and Dhananjay et al. for the n-ZnO/p-Si HJ diode [21,23]. The multistep tunneling process usually occurs at the HJ region of the n-ZnO matrix and p-Si substrate, which is attributed to the recombination of electrons, tunneling from ZnO into the empty gap states in the p-Si substrate, and holes, tunneling through the HJ barrier from the p-Si substrate to the n-ZnO matrix between the empty states [21,23]. Hence, our results show that the carriers in the Si QD-embedded ZnO thin film mainly transport via the ZnO matrix but not through Si QDs with direct, resonant, or phonon-assisted tunneling mechanisms, as reported for Si QDs embedded in the traditional matrix materials [24,25]. According to the multistep tunneling mechanism, the temperature dependence of I_s is given by the relation, $I_s \propto \exp(-E_a/kT)$, where E_a is the activation energy, k is Boltzmann's constant, and T is the absolute temperature [21,23]. Figure 6c shows the Arrhenius plot of $\ln(I_s)$ versus $1,000/T$. A linear relationship is clearly observed, which further confirms that the dominating carrier transport process is the multistep tunneling mechanism [19,21-23]. The E_a of around 0.37 eV obtained from the Arrhenius plot is a little larger than those of the reported n-ZnO/p-Si HJ diodes, which are usually smaller than 0.3 eV [19,21-23]. This means that the thermally activated

Figure 6 Carrier transport mechanism. (a) Forward *I-V* curves for different measurement temperatures, **(b)** the parameter B, and **(c)** Arrhenius plot of $\ln(I_s)$ versus $1,000/T$ for the Si QD-embedded ZnO thin film annealed at 700°C.

carriers are partially contributed from the embedded Si QDs since the intrinsic Si QDs can possess E_a larger than 0.4 eV [17,26]. Thus, we can conclude that the Si QDs embedded in ZnO matrix also contribute the carriers, and those carriers will partially escape from Si QDs into the ZnO matrix and transport inside. The largely improved resistivity suggests that the carriers transporting in the ZnO matrix can have a much better transport efficiency than those tunneling through barriers in the traditional matrix materials. With the unique carrier transport mechanism and better electrical properties, we believe that the Si QD thin films will have great potential for optoelectronic device application by using ZnO as matrix material.

Conclusions

In summary, we successfully fabricate a nc-Si QD-embedded ZnO thin film on a p-Si substrate using a ZnO/Si ML deposition structure. Our results indicate that the optical transmittance can be largely enhanced by increasing T_{ann} owing to the phase transformation of a- to nc-Si QDs embedded in the ZnO matrix, and up to about 90% transmittance in the long-λ range under a T_{ann} higher than 700°C is obtained. The Si QD-embedded ZnO thin film annealed at 700°C exhibits good diode behavior with a large rectification ratio of approximately 10^3 at ±5 V and significantly lower resistivity than that using the SiO_2 matrix material (10^4 times improvement). From temperature-dependent I-V curves, we find that the carriers transport mainly via the ZnO matrix, not through Si QDs, which is dominated by the multistep tunneling mechanism as in the n-ZnO/p-Si HJ diode. The unique transport mechanism differing from those using the traditional Si-based dielectric matrix materials can lead to much better carrier transport efficiency and electrical properties. Hence, we show that the Si QD thin film using the ZnO matrix material is very advantageous and has potential for optoelectronics device application.

References
1. Anopchenko A, Marconi A, Wang M, Pucker G, Bellutti P, Pavesi L: Graded-size Si quantum dot ensembles for efficient light-emitting diodes. Appl Phys Lett 2011, 99:181108.
2. Lin GR, Lin CJ, Lin CK, Chou LJ, Chueh YL: Oxygen defect and Si nanocrystal dependent white-light and near-infrared electroluminescence of Si-implanted and plasma-enhanced chemical-vapor deposition-grown Si-rich SiO2. J Appl Phys 2005, 97:094306.
3. Perez-Wurfl I, Hao X, Gentle A, Kim DH, Conibeer G, Green MA: Si nanocrystal p-i-n diodes fabricated on quartz substrates for third generation solar cell applications. Appl Phys Lett 2009, 95:153506.
4. Garoufalis CS, Zdetsis AD: High level ab initio calculations of the optical gap of small silicon quantum dots. Phys Rev Lett 2001, 87:276402.
5. Mirabella S, Agosta R, Franzò G, Crupi I, Miritello M, Savio RL, Stefano MAD, Marco SD, Simone F, Terrasi A: Light absorption in silicon quantum dots embedded in silica. J Appl Phys 2009, 106:103505.
6. Kang Z, Liu Y, Tsang CHA, Ma DDD, Fan X, Wong NB, Lee ST: Water-soluble silicon quantum dots with wavelength-tunable photoluminescence. Adv Mater 2009, 21:661–664.
7. Lin GR, Lin CJ, Kuo HC: Improving carrier transport and light emission in a silicon-nanocrystal based MOS light-emitting diode on silicon nanopillar array. Appl Phys Lett 2007, 91:093122.
8. Cheng CH, Lien YC, Wu CL, Lin GR: Mutlicolor electroluminescent Si quantum dots embedded in SiOx thin film MOSLED with 2.4% external quantum efficiency. Opt Express 2013, 21:391–403.
9. Lin GR, Pai YH, Lin CT, Chen CC: Comparison on the electroluminescence of Si-rich SiNx and SiOx based light-emitting diodes. Appl Phys Lett 2010, 96:263514.
10. Conibeer G, Green MA, Konig D, Perez-Wurfl I, Huang S, Hao X, Di D, Shi L, Shrestha S, Puthen-Veetil B, So Y, Zhang B, Wan Z: Silicon quantum dot based solar cells: addressing the issues of doping, voltage and current transport. Prog Photovolt Res Appl 2011, 19:813–824.
11. Özgür Ü, Alivov YI, Liu C, Teke A, Reshnikov MA, Dogan S, Avrutin V, Cho SJ, Morkoç H: A comprehensive review of ZnO materials and devices. J Appl Phys 2005, 98:041301.
12. Kuo KY, Hsu SW, Chuang WL, Lee PT: Formation of nano-crystalline Si quantum dots in ZnO thin-films using a ZnO/Si multilayer structure. Mater Lett 2012, 68:463–465.
13. Kuo KY, Hsu SW, Huang PR, Chuang WL, Liu CC, Lee PT: Optical properties and sub-bandgap formation of nano-crystalline Si quantum dots embedded ZnO thin film. Opt Express 2012, 20:10470–10475.
14. Cheng Q, Tam E, Xu S, Ostrikov KK: Si quantum dots embedded in an amorphous SiC matrix: nanophase control by non-equilibrium plasma hydrogenation. Nanoscale 2010, 2:594–600.
15. You JB, Zhang XW, Fan YM, Yin ZG, Cai PF, Chen NF: Effect of deposition conditions on optical and electrical properties of ZnO films prepared by pulsed laser deposition. Appl Surf Sci 2002, 197–198:363–367.
16. Sundaram KB, Khan A: Characterization and optimization of zinc oxide films by r.f. magnetron sputtering. Thin Solid Films 1997, 295:87–91.
17. Hao XJ, Cho EC, Scardera G, Shen YS, Bellet-Amalric E, Bellet D, Conibeer G, Green MA: Phosphorus-doped silicon quantum dots for all-silicon quantum dot tandem solar cells. Sol Energy Mater Sol Cells 2009, 93:1524–1530.
18. Di D, Xu H, Perez-Wurfl I, Green MA, Conibeer G: Improved nanocrystal formation, quantum confinement and carrier transport properties of doped Si quantum dot superlattices for third generation photovoltaics. Res Appl: Prog Photovolt 2013, 21:569–577.
19. Lee JD, Park CY, Kim HS, Lee JJ, Choo YG: A study of conduction of ZnO film/p-Si heterojunction fabricated by photoinduced electrodeposition under illumination. J Phys D Appl Phys 2010, 43:365403.
20. Mridha S, Basak D: Ultraviolet and visible photoresponse properties of n-ZnO/p-Si heterojunction. J Appl Phys 2007, 101:083102.
21. Zebbar N, Kheireddine Y, Mokeddem K, Hafdallah A, Kechouane M, Aida MS: Structural, optical and electrical properties of n-ZnO/p-Si heterojunction prepared by ultrasonic spray. Mater Sci Semicond Process 2011, 14:229–234.
22. Zhang Y, Xu J, Lin B, Fu Z, Zhong S, Liu C, Zhang Z: Fabrication and electrical characterization of nanocrystalline ZnO/Si heterojunctions. Appl Surf Sci 2006, 252:3449–3453.
23. Dhananjay, Nagaraju J, Krupanidhi SB: Investigations on zinc oxide thin films grown on Si (100) by thermal oxidation. Mater Sci Eng B 2007, 137:126–130.

24. Osinniy V, Lysgaard S, Kolkovsky V, Pankratov V, Larsen AN: **Vertical charge-carrier transport in Si nanocrystal/SiO$_2$ multilayer structures.** *Nanotechnology* 2009, **20**:195201.
25. Veettil BP: *Modelling and characterization of carrier transport through nanostructures.* PhD thesis. University of New South Wales, School of Photovoltaic and Renewable Energy Engineering; 2012.
26. Fangsuwannarak T: *Electronic and optical characterisations of silicon quantum dots and its applications in solar cells.* PhD thesis. University of New South Wales, Centre of Excellence for Advanced Silicon Photovoltaics and Photonics; 2007.